Benefits of switching from Si to SiC modules with further converter optimization

Antxon Arrizabalaga[1], Mikel Mazuela[1], Iosu Aizpuru[1], June Urkizu[1], Jon Aztiria[1]

[1] MONDRAGON UNIBERTSITATEA
Fundazioa eraikuntza; Jauregi Bailara, z.g, 20120
Hernani, Spain
Tel.: +34 / +(34) – 943794700.
E-Mail: aarrizabalaga@mondragon.edu
URL: https://www.mondragon.edu/

Keywords

«Wide bandgap devices», «DC-AC», «Switching losses», «Optimization», «Passive filters»

Abstract

SiC semiconductors have better characteristics than Si, improving power electronics converters performances. A prototype that can switch semiconductor technology without changing any other part of the system is built and tested, showing the efficiency improvements achieved with SiC. Finally, a theoretical system level converter optimization is done applying the experimental results.

Introduction

With the increased use of power electronics, the technical requirements of converters are also increasing [1], [2]. Higher power density, meaning less volume and less weight, as well as higher efficiency are needed. With higher integration of renewable energies, and switching devices connected to the grid, the waveform quality of inverters is also a concern nowadays [3]. Increasing the switching frequency can help in the filtering objective, without the need to increase the filter, which is one of the bulkiest parts of grid connected inverters [4].

In this aspect, state of the art silicon (Si) semiconductors have a natural technical limit [1], which directly affect to the converter performance, limiting the ability to reach the requisites of several applications. Silicon carbide (SiC) high power modules break the boundaries of Si, enabling higher power densities, with reduced size, weight and higher efficiency at converter level [5].

Fig. 1 shows the characteristics of SiC normalized to Si. As it is seen, SiC has a higher breakdown electric field, which allows to withstand higher voltage with a thinner drift layer, Fig: 2 (a), reducing the specific on resistance, and breaking Si boundaries, shown in Fig: 2 (b). In addition, the higher electron saturation velocity allows to switch from one switching state to other faster than Si [6], [7]. The faster switching means less switching losses, as it will be seen later.

When comparing Si and SiC 1700 V high power half bridge modules, the first difference is the transistor technology. For medium-high voltage and power levels, insulated gate bipolar transistors (IGBT) are used with Si, while the higher breaking voltage of SiC allows to form metal oxide-semiconductor field-effect transistors (MOSFET). These transistors do not suffer from the direct voltage drop that IGBTs suffer, showing better conduction performance in low currents. The second main difference occurs in the switching, in which MOSFETs do not have a tail current in the turn off. In addition, the faster switching of the SiC with respect to Si makes the switching of SiC MOSFETs more efficient.

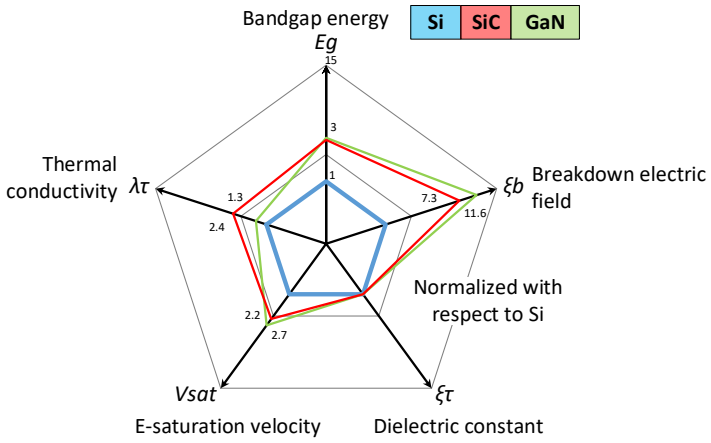

Fig. 1: Key normalized electrical and thermal characteristics of Si , GaN and SiC, [8].

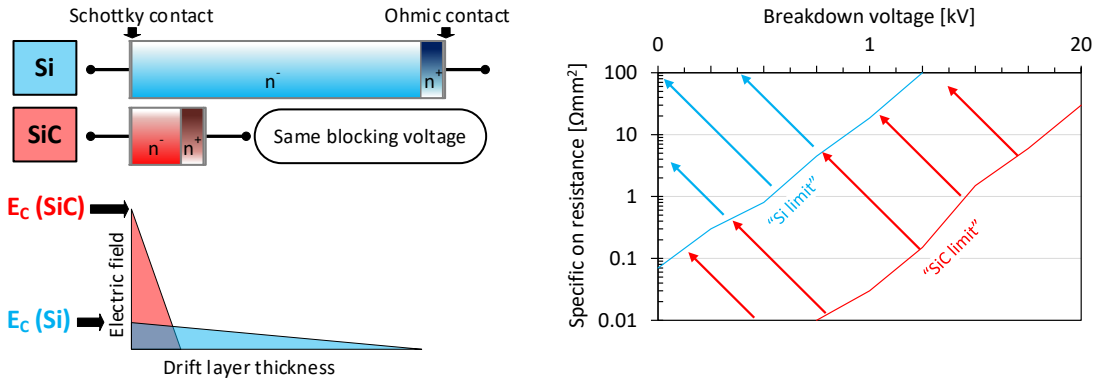

(a) (b)

Fig: 2: SiC and Si characteristic comparison, (a) drift layer thickness for same blocking voltage, (b) specific on-resistance vs breakdown voltage, [6].

The previously mentioned better performance leads to an improved efficiency of the converter. This can lead to smaller cooling systems (CS), reducing the volume of the converter [9], [10], so it can help to meet the most restrictive requirements in several applications [11]–[13]. Renewable energy can be one of those applications, reducing the volume of the photovoltaic (PV) inverter for example, being able to install it in the rooftops of residential buildings [14]. Another industrial application for the improvements SiC brings to power electronics is the electric vehicle (EV) [5]. A smaller layout of the converter can allow new locations for inverters in the electric cars, and higher power density will allow to have more power transmitted to the mechanical shaft, improving the overall performance of the EVs [5].

This paper presents an experimental verification of the efficiency improvements achieved by switching from Si to SiC technology. The experimental platform has been designed to replace Si and SiC modules in the same system, in order to get a fair comparison of the device performance. However, an optimized converter is required to maximize the benefits of SiC modules.

Experimental platform

This section presents the designed prototype. The objective is to analyze the effect of replacing the state of the art Si technology with high power SiC modules. The same power stage, with the same components are used, replacing only the semiconductors. This approach isolates the impact of the technology in the efficiency of the converter. To make a fair comparison, the tests are performed in a controlled environment using passive loads. This allows to test both technologies under the same operation points and conditions.

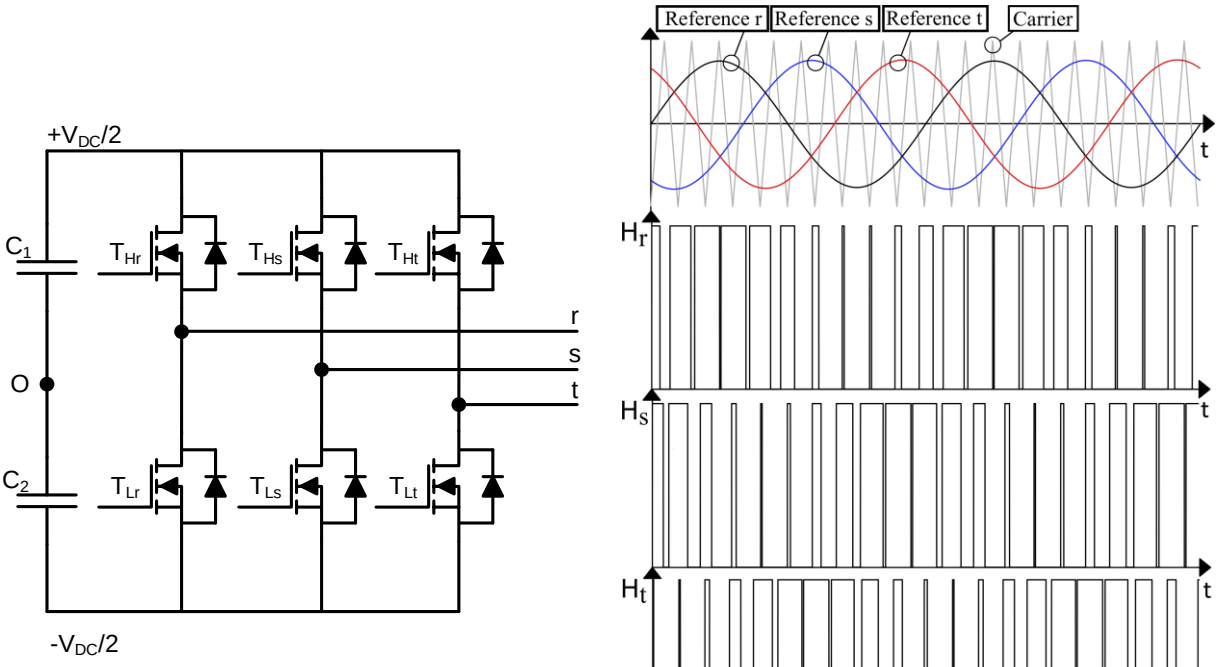

(a) (b)

Fig. 3: Three phase two level converter, (a) topology scheme and (b) PWM modulation diagram with gate driving signals for each phase.

The 3 phase 2 level (2L) topology is selected, and shown in Fig. 3 (a). Fig. 3 (b) shows the driving PWM modulation. The reference of each phase is 120º out of phase. High and low switches are complementary, and represented with *H* and *L* in Fig. 3. Only the driving signal of the high switch is shown per phase.

Converter design

The key components of the converter design are the semiconductor modules. Si and SiC modules must have the same package, in order to be replaceable. The universal 62 mm module is selected. The main characteristics of the selected modules are shown in Fig. 4, together with the pinout. Fig. 5 shows the designed converter. By taking out the DC link capacitors and the drivers, all fixed to the busbar, the lower layer of the converter is accessible. The design ensures the module replacement is done in a fast and safe way, allowing to test both Si and SiC technologies efficiently.

Technology	**Si IGBT**	**SiC MOSFET**
Reference	FF300R17KE4	FF8MR20KM1*
I_C-I_D	300 A	185 A
V_{CE}-V_{DS}	1700 V	2000 V
*Under development, preliminary samples.		

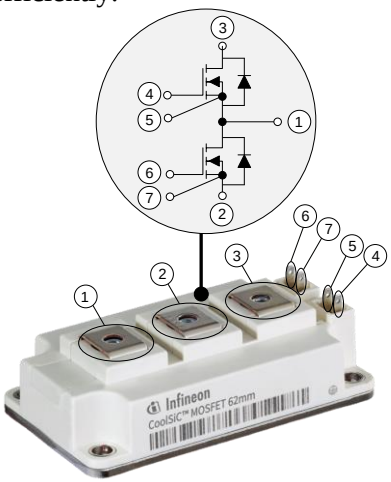

(a) (b)

Fig. 4: Selected 62 mm modules, (a) Characteristics, (b) package pinout.

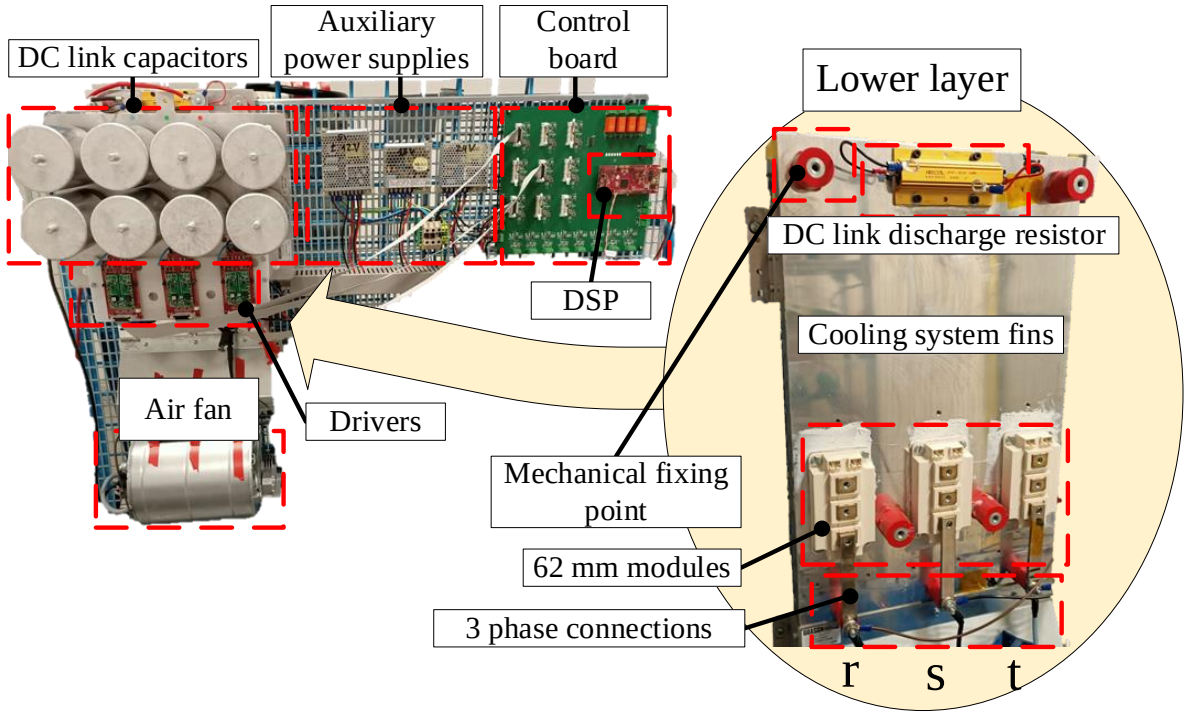

Fig. 5: The designed converter, with the replaceable 62 mm modules in the lower layer.

Table I: List of the components used in the power stage.

Component	Reference	Qty	Detail
Drivers	2ASC-17A1HP	3	Compatible for Si and SiC.
DC link capacitors	947D102K901CJRSN	8	900 V and 1 mF each.
Discharge resistor	HS150 18K	1	18 kΩ and 150 W.
Busbar	Own design	1	Custom made.
Cooling system	SC-C300P	1	Radial 35 m^3/min forced airflow.
DSP	Delfino C2000	1	High resolution PWM.
Control board	Own design	1	8 analog measurements. 9 conditioned driving signals. 4 external relays for security circuit breakers.
DC power supply	Yaskawa 4A0100	1	Regenerative power converter with 150 A DC current.

Table I shows the components used to build the common power stage. The same drivers can work with Si and SiC, with a maximum voltage of 2000 V in the DC link. The DC link capacitors are set in 4 parallel branches of 2 capacitors in series. With this configuration, high voltage capability of the converter is ensured, as well as having high capacitance in the DC link. A discharge resistor is installed as a security measure, to ensure the capacitors are discharged when the converter is turned off. The custom made busbar connects all the before mentioned components, giving them mechanical stability. If the busbar is removed, all the attached components are also removed, making the lower layer of the converter easily accessible.

The control board is an own design, interfacing between the digital signal processor (DSP) and the drivers. It also allows to perform 8 different measurements and drives the security circuit breakers with 4 relays. The control is implemented in MatLab-Simulink and deployed to the DSP. Finally, a regenerative power converter, also supplying the power, sets the DC voltage.
The designed power converter has a rated power of 125 kVA. However, the grid in the testing facility can only provide less than 50 kVA. Testing the converter at higher power in another facility is a future objective.

Test results

The tests are performed keeping the same fixed DC link voltage and modulation index m_a. The active power is increased from 5 to 40 kW, reaching the limit of the testing facility. The load inductors are changed in every testing point, to ensure the power factor PF is kept between the desired margins. The fundamental frequency f_0 of the synthesized sinewave is fixed in order to get the necessary impedance with the available load inductors. The switching frequency is varied from 2.5 to 10 kHz, to evaluate its effect in both technologies. Table II shows the testing conditions and operation points. The same points are repeated for both Si and SiC modules, in order to make a fair comparison.

The converter is run in the operation conditions previously described. The obtained line voltage and phase currents are shown in Fig. 8 for the SiC modules at full power. Only two phases are measured because it is a balanced system. The peak current value in this test is 110 A, corresponding to 40 kW.

Efficiency tests

First, both technologies are tested in all the power range at 2.5 kHz switching frequency, Fig. 6 (a). Even if the low switching frequency favors Si modules, the converter with SiC has better efficiency in all the power range. The efficiency difference is the highest at low power, where switching losses dominate over the conduction losses. At high power, the efficiency gap is smaller, due to the better conduction characteristics of the Si IGBTs at high current. However, the Si converter does not reach 98 %, while the SiC converter goes over 99 %.

Fig. 6 (b) presents the efficiency of both technologies at maximum power (40 kW), but different switching frequencies. It is observed how the SiC converter keeps high efficiency, over 98.8 % even at 10 kHz, while its Si counterpart drops below 94.5 %. This result shows the possibility to increase the switching frequency with SiC power modules and still keep high efficiency. The switching frequency increment allows improving other components of the system, such as the filters.

Table II: Test operation points for both Si and SiC modules.

Parameter	Value	Unit
DC voltage	630	V
Modulation index	0.9	/
Power factor	0.75-0.85	/
Fundamental frequency	250	Hz
Switching frequency	2.5-10	kHz
Active power	5-40	kW

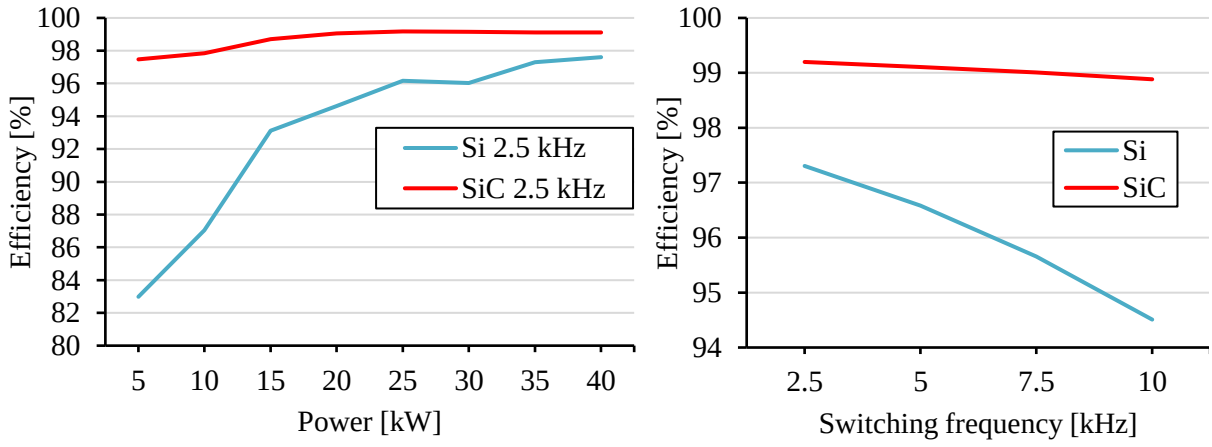

(a) (b)

Fig. 6: Efficiency test results for both Si and SiC technologies, (a) at 2.5 kHz switching frequency and all the power range, (b) at maximum power and different switching frequencies.

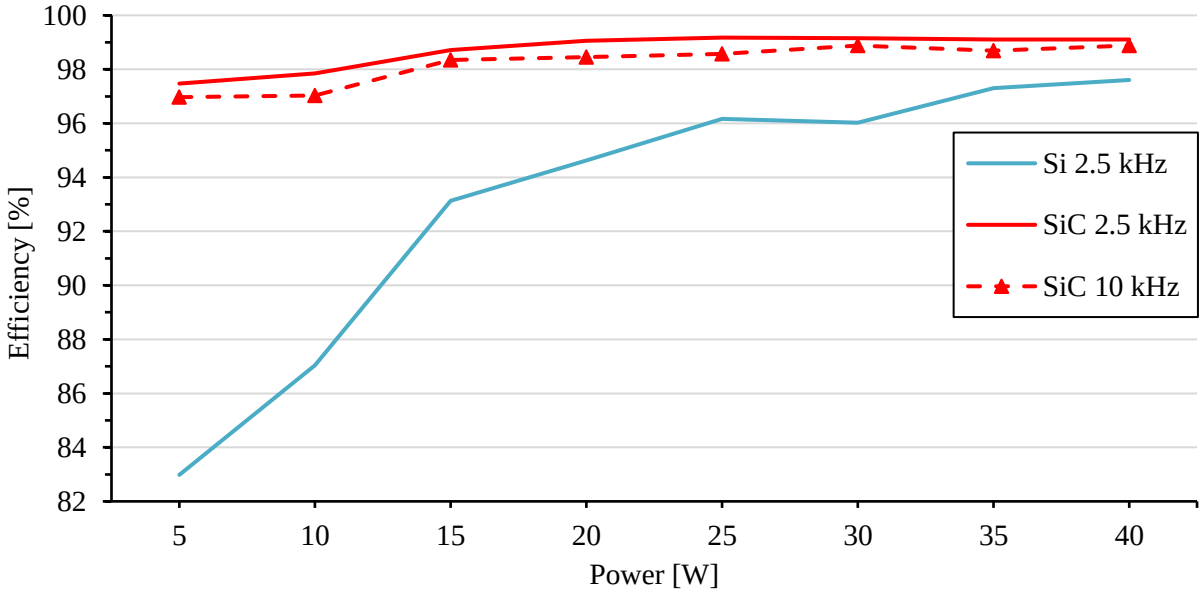

Fig. 7: Efficiency test results for both Si and SiC technologies in all the power range, including SiC at 10 kHz switching frequency.

Fig. 7 includes the efficiency of the SiC technology at 10 kHz switching frequency in all the power range. Although the increased switching frequency penalizes efficiency, the evolution is similar to the 2.5 kHz system, and still achieves high values. The worst point is at low power, but the efficiency is kept over 95 %. The highest value is 98.88 %, only losing 0.22 % with respect to the system at 2.5 kHz.

The output waveforms of the converter with SiC modules are shown in Fig. 8. The waveforms in Fig. 8 (a) are obtained at low switching frequency, 2.5 kHz. The ones in Fig. 8 (b) are obtained at 10 kHz switching frequency. The better output waveform quality is visible in the high switching frequency case, both for the line voltage and phase current. With an improved output waveform such as the one in Fig. 8 (b), the filtering needs are reduced. This directly impacts the total volume of the converter, as it is studied in the next section.

Converter volume optimization

The cooling system used for the tests in the previous section is oversized for security reasons. Thus, a theoretical converter volume optimization can be performed, based on the efficiency test results obtained in the previous section. The cooling systems and the required filters volumes are compared for Si and SiC technologies. In the case of the SiC, the increase in the switching frequency is also considered. The analysis shows the possible converter volume reduction with the use of SiC technology.

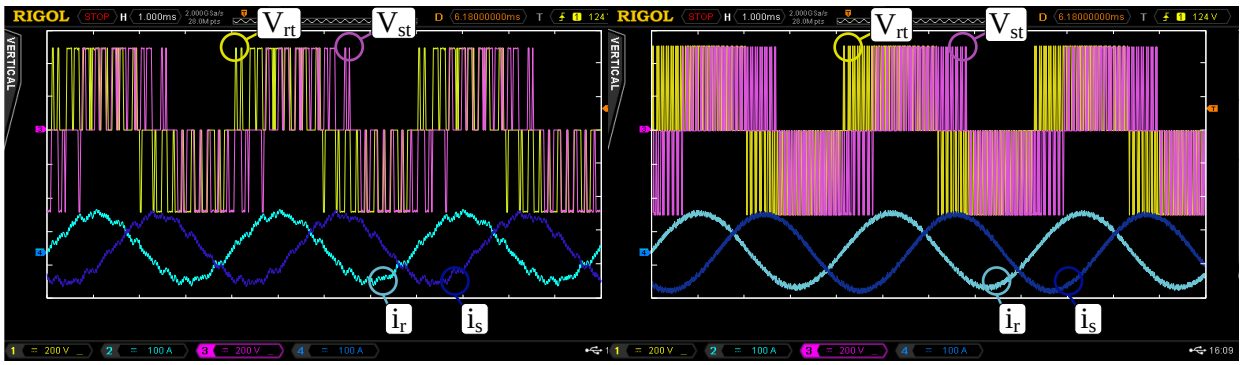

(a) (b)

Fig. 8: Line voltage and phase current of the SiC converters at 40 kW, (a) at 2.5 kHz switching frequency, (b) at 10 kHz.

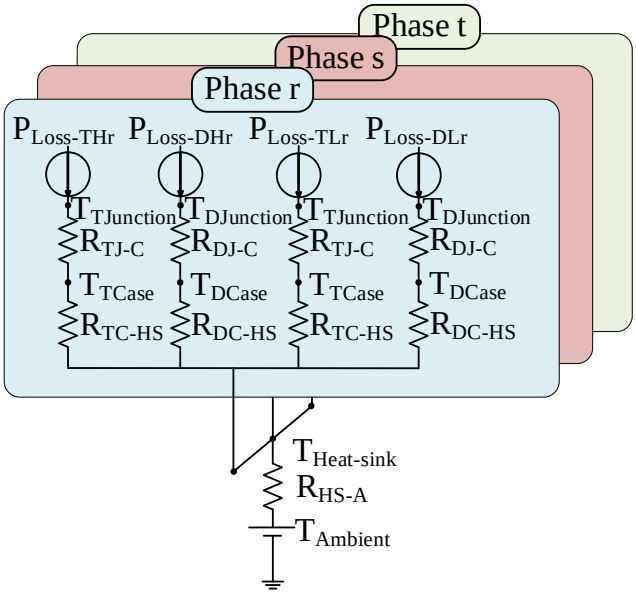

(a)

Parameter	Si	SiC 2.5 kHz	SiC 10 kHz
$T_{Junction}$	125 ºC	125 ºC	125 ºC
$T_{Ambient}$	20 ºC	20 ºC	20 ºC
P_{Loss}	1424 W	320 W	465 W
$R_{HS\text{-}A\ Max}$	0.0436 ºC/W	0.2931 ºC/W	0.1908 ºC/W

(b)

Fig. 9: Cooling system analysis, (a) equivalent thermal circuit, (b) most relevant parameters.

Cooling system calculation

Fig. 9 shows the analysis of the cooling system. First, the equivalent thermal circuit is drawn, Fig. 9 (a), paralleling the modules in phase r, s and t. Each module has two semiconductors, high H and low L, and each semiconductor a transistor T and a diode D. R_{J-C} and R_{C-HS} represent the thermal resistance from the junction to the case and from the case to the heat-sink respectively. These parameters are found in the datasheets of the modules. Maximum junction temperature and ambient temperature are shown in Fig. 9 (b). The power losses are the maximum registered for each configuration, in the tests shown in Fig. 7, and presented in Fig. 9 (b). As it is not possible to measure if the losses are generated in the diode or in the transistor, the worst case scenario is analyzed. This is when all the losses are generated in the path with the highest R_{th}. The maximum allowable thermal resistance of the cooling system R_{HS-A} is calculated for each case.

Next, commercial cooling systems are plotted in Fig. 10, depending on their volume and thermal resistance. For high thermal resistances, axial air fans are enough, while for low thermal resistances, high volume is required together with radial air fans. A trend approximating the volume of the cooling system depending on the thermal resistance is calculated (1), and shown with a black dashed line in Fig. 10.

$$Vol_{CS} = 0.3622 \cdot {R_{th}}^{-0.988} \quad (1)$$

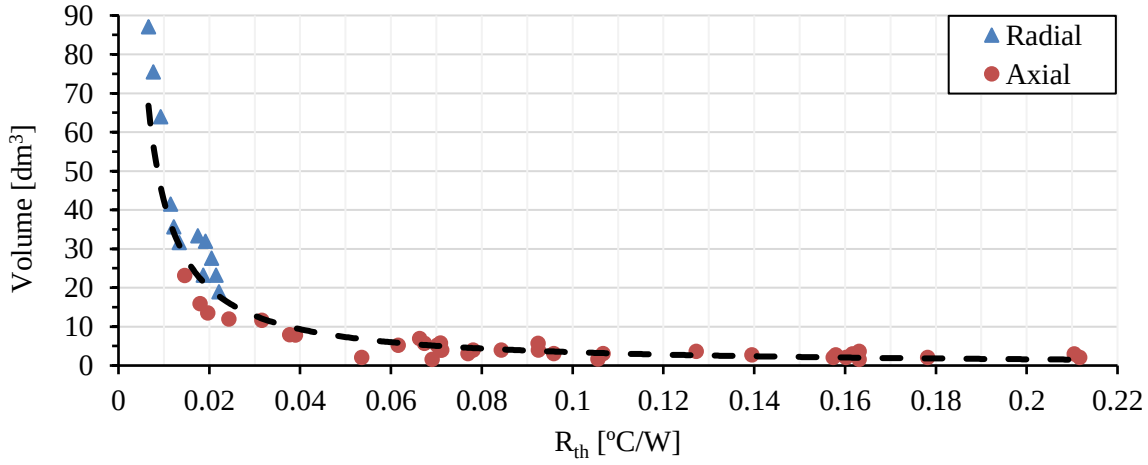

Fig. 10: Commercial cooling systems depending on their thermal resistance and volume, with the calculated potential trend in black.

Filter volume calculation

An LC line filter is usually added in the output of the converter to shape the output current. The inductance and capacitance values in the filter are calculated using expressions (2) and (3) presented in [15] and [16] respectively. V_{dc} is 630 V , ΔI_{out} is defined as 10 % of the I_{out} and Att_{req}, which refers to the required attenuation of the filter, is set to 0.01 in order to have enough damping in the switching frequency [17]. m refers to the converter topology level, 2 in this case.

$$L_f = \frac{V_{dc}}{6(m-1) \cdot \Delta I_{out} \cdot f_{sw}} \tag{2}$$

$$C_f = \frac{1}{(2\pi \cdot f_{sw})^2 \cdot L_f \cdot Att_{req}} \tag{3}$$

To calculate the volume of the inductor, the area product A_p technique proposed in [18] is used. Equation (4) uses the factor k_L to relate the area product and inductor volume. As this factor is dependent on the switching frequency, a polynomial approximation is performed to calculate k_L in [19], and shown in (5). In the case of the capacitor, [16] identifies a relation between volume, the rated voltage and capacitance for every technology. To estimate the required volume, commercial foil capacitors are analyzed, considering their volume and rated voltage, Fig. 11 (a). It is identified that the volume is linearly dependent on the rated capacitance, for a same rated voltage. 800 V series is selected, and the linear expression shown in (6), represented with a black dashed line in Fig. 11(a), is used to estimate the required capacitors' volume in the filter, introducing the capacitance value C_f in micro farads (µF). Fig. 11 (b) shows the volume of the required LC filter for each switching frequency. (7) shows the whole filter volume calculation. After adding the volumes of the capacitor and the inductor, the total volume is multiplied by three in order to consider the three phases of the converter.

$$Vol_{L_f} = k_L \cdot A_p{}^{\frac{3}{4}} \tag{4}$$

$$k_L = 2.676 \times 10^{-5} \cdot f_{sw} + 19.71 \tag{5}$$

$$Vol_{C_f} = 0.0016 \cdot C_f + 0.0062 \tag{6}$$

$$Vol_{Filter} = 3 \cdot (Vol_{C_f} + Vol_{L_f}) \tag{7}$$

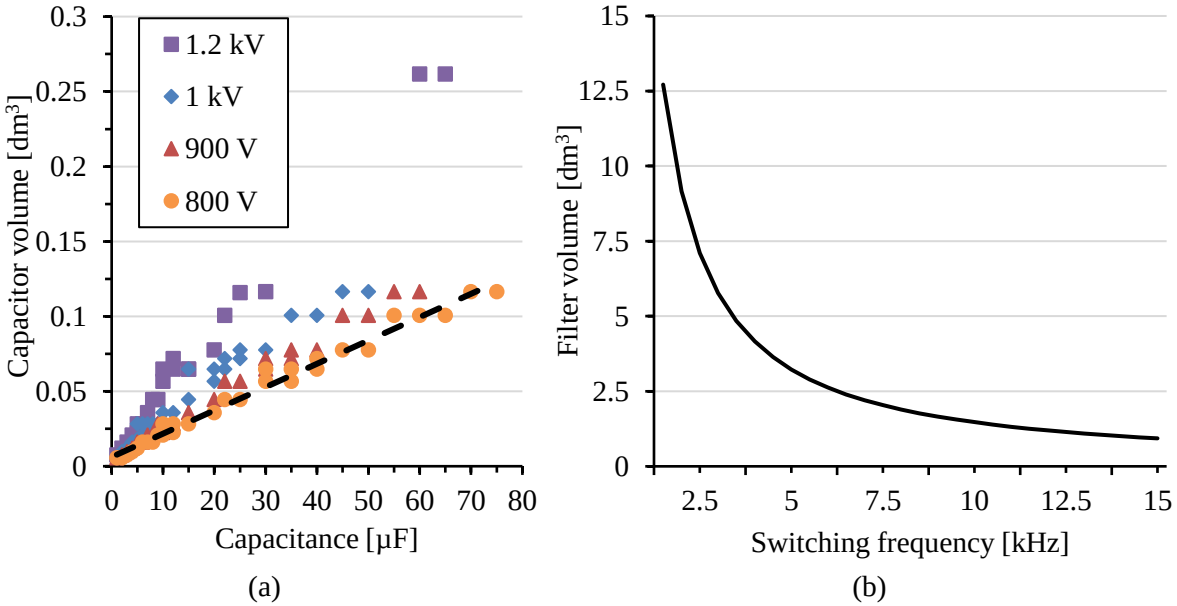

Fig. 11: Volumes of, (a) commercial capacitors, (b) whole filter.

Table III: optimized converter characteristics, with the use of SiC.

	Si at 2.5 kHz	SiC at 2.5 kHz	SiC at 10 kHz	Unit
Experimental efficiency at nominal power	97.60	99.19	98.88	%
Required CS volume	8.00	1.21	1.86	dm^3
Required CS volume reduction	/	84.87	76.75	%
Required filter volume	7.10	7.10	1.47	dm^3
Required filter volume reduction	/	/	79.29	%
Combined volume	15.1	8.31	3.33	dm^3
Combined volume reduction	/	44.96	77.94	%

Combined volume analysis

Finally, the cooling system and the filter volume are added for each case, to calculate the combined volume of the converter. Table III shows the results, being SiC at 10 kHz the solution that would provide the best volume reduction. The better efficiency of the SiC devices allow to reduce the cooling system compared to the Si converter. Finally, and due to the good switching performance of SiC, increasing the switching frequency does not increase the losses considerably, keeping the cooling system volume low.

If the switching frequency is increased in the SiC converter, the filter can also be reduced, and the combined volume reduction is maximum. The efficiency of the optimized SiC converter is still as high as 98.88 %.

Conclusion

A functional inverter is presented in this work, having the capability to change the semiconductor technology from Si IGBTs to SiC MOSFETs while keeping the rest of the system unchanged, see Fig. 5. This provides the possibility to compare the semiconductor technologies in a fair way. The results in efficiency are shown, improving 1.59 % at nominal power, Fig. 6 (a). In addition, the evolution of the efficiency is analyzed when the switching frequency is increased, Fig. 6 (b). Taking advantage of the better switching performance of the SiC MOSFETs, it is observed that the switching frequency can be increased from 2.5 kHz to 10 kHz and still improve the efficiency of the state of the art Si converter 1.28 %.

The whole system should be optimized in order to fully use the SiC semiconductor capabilities. This optimization is shown in Table III, achieving 77.94 % combined volume reduction with SiC MOSFETs switching at 10 kHz, while the efficiency at nominal power is still improved, as mentioned before. In addition, reducing the filter 79.29 % is found valuable, because the cost and weight of the filter are a significant part of the whole converters.

The advantages of migrating from Si IGBTs to SiC MOSFETs are experimentally proved in a general purpose inverter. A theoretical converter optimization is performed, achieving valuable improvements at system level; that can be applied to meet the restrictive requirements some applications are demanding nowadays. The improved system could easily benefit electric vehicles, with its reduced volume and weight, as well as domestic PV systems, by allowing to install inverters attached to solar panels in rooftops, for example.

References

[1] M. F. Yaakub, M. A. M. Radzi, F. H. M. Noh, and M. Azri, “Silicon carbide power device characteristics, applications and challenges: An overview,” Int. J. Power Electron. Drive Syst., vol. 11, no. 4, pp. 2194–2202, 2020.

[2] H. Zhang and L. M. Tolbert, “Efficiency Impact of Silicon Carbide Power Electronics for Modern Wind Turbine Full Scale Frequency Converter,” IEEE Trans. Ind. Electron., vol. 58, no. 1, 2011.

[3] F. Blaabjerg and K. Ma, “Wind energy systems,” Proc. IEEE, vol. 105, no. 11, pp. 2116–2131, 2017.

[4] J. W. Kolar et al., “Impact of Magnetics on Power Electronics Converter Performance State-of-the-Art and Future Prospects Magnetics Committee,” Zurich, 2017.

[5] A. Matallana et al., “Power module electronics in HEV/EV applications: New trends in wide-bandgap semiconductor technologies and design aspects,” Renew. Sustain. Energy Rev., vol. 113, no. June, p. 109264, 2019.

[6] T. Kimoto, “Material science and device physics in SiC technology for high-voltage power devices,” Jpn. J. Appl. Phys., vol. 54, no. 4, 2015.

[7] D. Garrido, “Impacto de los semiconductores de banda ancha prohibida en el diseño de convertidores de potencia,” Mondragon Unibertsitatea, 2019.

[8] B. W. Williams, Principles of Power electronics. Glasgow: Barry W. Williams, 2006.

[9] H. Zhang, L. M. Tolbert, and B. Ozpineci, “Impact of SiC devices on hybrid electric and plug-in hybrid electric vehicles,” IEEE Trans. Ind. Appl., vol. 47, no. 2, pp. 912–921, 2011.

[10] E. Gurpinar, “Wide-Bandgap Semiconductor Based Power Converters for Renewable Energy Systems,” Univ. Nottingham, 2017.

[11] A. Castellazzi, E. Gurpinar, Z. Wang, A. S. Hussein, and P. G. Fernandez, “Impact of wide-bandgap technology on renewable energy and smart-grid power conversion applications including storage,” Energies, vol. 12, no. 23, pp. 1–14, 2019.

[12] A. S. Abdelrahman, Z. Erdem, Y. Attia, and M. Z. Youssef, “Wide Bandgap Devices in Electric Vehicle Converters: A Performance Survey,” Can. J. Electr. Comput. Eng., vol. 41, no. 1, pp. 45–54, Dec. 2018.

[13] C. Sintamarean, E. Eni, F. Blaabjerg, R. Teodorescu, and H. Wang, “Wide-band gap devices in PV systems - Opportunities and challenges,” in 2014 International Power Electronics Conference, IPEC-Hiroshima - ECCE Asia 2014, 2014, pp. 1912–1919.

[14] A. Singh et al., “Development and Validation of a SiC Based 50 kW Grid-Connected PV Inverter,” 2018 IEEE Energy Convers. Congr. Expo. ECCE 2018, no. September, pp. 6165–6172, 2018.

[15] M. Mazuela, “Análisis y desarrollo de una novedosa topología de convertidor multinivel para aplicaciones de media tensión y alta potencia,” Mondragon Unibertsitatea, 2015.

[16] J. W. Kolar et al., “PWM converter power density barriers,” Fourth Power Convers. Conf. PCC-NAGOYA 2007 - Conf. Proc., no. May, 2007.

[17] A. Anthon, Z. Zhang, M. A. E. Andersen, D. G. Holmes, B. McGrath, and C. A. Teixeira, “The benefits of SiC mosfets in a T-type inverter for grid-tie applications,” IEEE Trans. Power Electron., vol. 32, no. 4, pp. 2808–2821, 2017.

[18] W. G. Hurley and W. H. Wölfle, "Transformers and inductors for power electronics: theory, design and applications". Wiley-Blackwell, 2013.

[19] E. Gurpinar and A. Castellazzi, “Single-Phase T-Type Inverter Performance Benchmark Using Si IGBTs, SiC MOSFETs, and GaN HEMTs,” IEEE Trans. Power Electron., vol. 31, no. 10, pp. 7148–7160, Oct. 2016.